J. Membrane Biol. 77, 1–14 (1984)

The Journal of
Membrane Biology

Electrical Coupling Between Cells in Islets of Langerhans from Mouse

G.T. Eddlestone*, A. Gonçalves**, J.A. Bangham and E. Rojas
Department of Biophysics, School of Biological Sciences, University of East Anglia, Norwich NR4 7TJ, England

Summary. Two microelectrodes have been used to measure membrane potentials simultaneously in pairs of mouse pancreatic islet cells. In the presence of glucose at concentrations between 5.6 and 22.2 mM, injection of current i into cell 1 caused a membrane potential change in this cell, V_1, and, provided the second microelectrode was less than 35 μm away, in a second impaled cell 2, V_2. This result establishes that there is electrical coupling between islet cells and suggests that the space constant of the coupling ratio within the islet tissue is of the order of a few β-cell diameters. The current-membrane potential curves $i - V_1$ and $i - V_2$ are very similar. By exchange of the roles of the microelectrodes, no evidence of rectification of the current through the intercellular pathways was found. Removal of glucose caused a rapid decrease in the coupling ratio V_2/V_1. In steady-state conditions, the coupling ratio increases with the concentration of glucose in the range from 0 up to 22 mM. Values of the equivalent resistance of the junctional and nonjunctional membranes have been estimated and found to change with the concentration of glucose. Externally applied mitochondrial blockers induced a moderate increase in the junctional resistance possibly mediated by an increase in intracellular Ca^{2+}.

Key Words β-cells · electrical coupling · islets of Langerhans · cell-to-cell coupling · intercellular communication

Introduction

The majority of studies on the electrophysiology of the islet of Langerhans used a high resistance glass microelectrode to impale a single cell to monitor the membrane potential (Dean & Matthews, 1968, 1970*a*,*b*; Matthews & Sakamoto, 1975*a*,*b*; Meissner, 1976*a*; Atwater, Ribalet & Rojas, 1978, 1979*b*; Atwater, Dawson, Ribalet & Rojas, 1979*a*; Ribalet & Beigelman, 1979, 1980). It was implicitly assumed in these studies that the potential records obtained using this method were representative of the electrical activity of the islet β-cell population as a whole. Some evidence to support this assumption has been presented by Meissner (1976*b*) who used pairs of microelectrodes to simultaneously impale two cells within the same islet. This study showed that the glucose-induced bursts of electrical activity of the cells within the individual islet are in synchrony.

Morphological studies have shown that the β-cell membrane in the rat contains gap junctions (Orci, Unger & Renold, 1973; Meda, Perrelet & Orci, 1979), these being plaques of sub-units, or connexons, each of which surrounds a pore which connects adjacent cells. Furthermore, recently Michaels and Sheridan (1981) have microinjected Lucifer yellow into a rat pancreatic islet cell and observed that there is transfer of the dye to neighboring cells. This result together with experiments on the transfer of glycolytic substrates between cells in monolayer culture derived from rat islets (Kohen, Theorell, Mintz & Rabinovitch, 1979) strongly support the hypothesis that the cells within an islet function in concert as the gap junction is thought to represent an intercellular pathway for small molecules (for review *see* Loewenstein, 1981).

It has been suggested that the permeability of the junction may be correlated to the intracellular free ionized calcium level (Rose & Loewenstein, 1975, 1976; Rose, Simpson & Loewenstein, 1977; Rose & Rick, 1978) or to the intracellular pH (Turin & Warner, 1977, 1980).

This study was undertaken to establish whether electrical coupling of pancreatic β-cells occurs and, if so, whether it was affected by glucose and mitochondrial inhibitors known to induce an increase in cytosolic calcium (Rojas & Hidalgo, 1968).

An abstract with some aspects of this work has been published elsewhere (Eddlestone & Rojas, 1980).

Present address: *Department of Medicine, University of Southern California School of Medicine, Los Angeles. **Departamento de Fisiologia y Biofisica, Instituto de Biologia, UNICAMP, 13,100 Campinas, S. P., Brazil.

Materials and Methods

Preparation and Chamber

Two- to five-month-old albino mice were used in this study. Prior to use in experiments the mice were allowed free access to food and water.

In the pancreases used, the islets varied in diameter from less than 100 to about 600 μm. Islets were dissected from the pancreas with a surrounding of acinar tissue. A piece of pancreas with a few islets was rapidly transferred to the experimental chamber, where it was fixed to the silicon rubber base with fine steel pins through the acinar tissue. During this procedure, the chamber was perfused with Krebs solution with 2.8 mM glucose at 37°C. The chamber volume was 0.3 cm^3 and the solution flow rate was 1.4 cm^3 per minute.

Recording System

Two modes of signal recording were used. In the differential mode the potential was measured between a pair of Ag/AgCl half-cells (one within the microelectrode, and the second, in the Krebs solution, connected to the solution in the chamber by a Krebs-agar bridge). In the nondifferential recording mode the potential difference was measured between an Ag/AgCl half-cell in the microelectrode and an earthed Ag/AgCl half-cell in the experimental chamber. Using this latter mode of recording, current-injection was possible (*see* Fig. 1 in Atwater, Dawson, Eddlestone & Rojas, 1981). The two modes of recording could be switched between the pair of microelectrodes such that both membrane potentials could be measured accurately and either cell could be injected with current.

The differential and nondifferential outputs from the amplification system were displayed on a dual beam oscilloscope and fed to a four-channel magnetic tape recorder (Store 4, Racal Thermionic Ltd. or Tandberg, Series 115) for permanent recording. The tape recorder output was fed to a dual-channel chart recorder (Bryans Southern Instruments, Model 2800) which provided a record of the protocol.

The functioning of the current injection circuit has been considered before (for circuit *see* Fig. 1 in Atwater et al., 1981). The gain of the feedback loop (amplifiers 3 and 5 in Fig. 1 of Atwater et al., 1981) is critical as it determines the linearity of the system. This and the calibration of the current pulse magnitude were checked using a current-to-voltage transducer in the 10^{-12} amp range. The current output was adjusted to 0.22×10^{-9} amps/volt and was shown to remain constant throughout the microelectrode resistance range used in the experiments (from 150×10^6 to 350×10^6 Ω). In the absence of a stimulating voltage the current output was below the limit of detection.

The null-bridge (amplifier 7 in Fig. 1 of Atwater et al., 1981) allows the subtraction from the output signal of the fraction of the voltage deflection due to the passage of injected current through the resistance of the microelectrode. The subtraction is set up as follows. With the microelectrode in solution, a voltage pulse is applied to amplifier 4. In the absence of compensation the expected ohmic voltage deflection is observed at the output of amplifier 7. By increasing the proportion of the signal reaching the inverting input of the null-bridge this deflection can be subtracted, leaving only the capacity transients (no capacity compensation was built into this apparatus). Upon penetrating the cell the voltage deflection caused by injected current pulses should be due only to the cell input resistance R_A. It should be noted that this is only true if the microelectrode tip resistance does not change during the penetration of the cell membrane.

Electrodes

Thick glass capillaries of external diameter 2 mm and internal diameter 1 mm with a 0.1 mm diameter-filling fiber were used for the production of microelectrodes. These were filled with 50% 3 M KCl, 50% 2 M potassium citrate mixture. The electrode resistance suitable for work on islet cells was limited to the range from 150×10^6 to 250×10^6 Ω. Below this range the electrode disturbed the surface of the tissue, causing a depression prior to penetration and, while this was not particularly significant in single electrode experiments, it made dual penetrations impossible. With resistance above 250×10^6 Ω the electrodes were prone to bending, giving spurious potential changes, and also blockage.

The rectifying properties of the electrodes were investigated by injection of current of different magnitudes and polarities. Electrodes were tested from different batches at random, for currents in the range from −0.2 to 0.2 nA, and in no case was rectification apparent.

Estimation of Interelectrode Distance

Each electrode was held in a perspex holder by a 3-mm internal diameter coil spring giving interference fit. The microelectrode holders were carried by micromanipulators. One manipulator was mounted vertically, the other at an angle of 7° from vertical to allow the electrodes to be brought close together without interference between their carriers. The final approach to the tissue with the electrodes was observed under 100× magnification. All impalements were made close to the surface of the islet. Final coordination of the electrode across the field of vision was relatively simple, but coordination in and out of the plane of vision was more difficult, requiring the use of the microscope fine focus to ascertain whether the electrode tips were in the same plane of focus.

Solutions

Throughout this study a modified Krebs-Ringer's Bicarbonate (KRB) solution was used. The composition of the solutions is given in Table 1. In experiments involving variation of potassium concentration Na-KRB and K-KRB were produced and mixed to give the required potassium concentration.

Results

Current injection has previously been used to investigate the input resistance R_A of the pancreatic β-cell (Matthews & Sakamoto, 1975*a*,*b*; Atwater et al., 1978, 1979*a*,*b*; Ribalet & Beigelman, 1979). In this study the technique was extended to investigate both cell input resistance and intercellular current spread and thereby the degree of electrical coupling

Table 1. Composition of solutions

Name	NaCl	KCl	$NaHCO_3$ (mM)	$CaCl_2$	$MgCl_2$
KRB	120	5	25	2.56	1.13
Na-KRB	125	—	25	2.56	1.13
K-KRB	—	125	25	2.56	1.13

FCCP was added to the KRB from 50 μM FCCP/ethanol stock solution. Quinine was added from 10 mM quinine stock solution.

between cells. The injected cell was defined as cell 1, the noninjected cell as cell 2, such that a current pulse applied to cell 1 gave rise to a voltage deflection in each of the two impaled cells referred to as V_1 and V_2, respectively. The relation V_2/V_1, the coupling ratio, was taken as an index of intercellular communication.

Pairs of microelectrodes were used to monitor electrical activity simultaneously in two cells within the same islet of Langerhans. With the two electrodes in solution and a tip separation of 20 μm, 0.2 nA rectangular current pulses were applied through microelectrode 1. There was no perceptible response in the record of the output from microelectrode 2 (except for small capacity transients). With microelectrode 1 in a cell responding to 11 mM glucose with the typical bursts of electrical activity, microelectrode 2 was positioned close to the islet surface and to microelectrode 1. Current pulses of 0.2 nA through microelectrode 1 produced no response in the output from microelectrode 2, except capacity transients. A similar result was obtained when current was passed extracellularly with microelectrode 2 recording from within a cell.

This sequence of control experiments was repeated on several occasions at the beginning and end of dual electrode impalement experiments and on no occasion was there a response from microelectrode 2 when injecting current through microelectrode 1.

These control experiments show that V_2 can be attributed to current flowing through the cell system of the islet of Langerhans.

Initially experiments were performed in the presence of glucose with the two microelectrodes in active cells 35 to 100 μm apart. Current pulses were then injected into cell 1. The results from one of these experiments are illustrated in Fig. 1.

The Figure shows records of the membrane potential changes in two cells in response to 11.1 mM glucose. A segment of the records (indicated in the upper part) is shown in the lower part using an expanded time base to illustrate that although the burst patterns of both cells occurred at the same

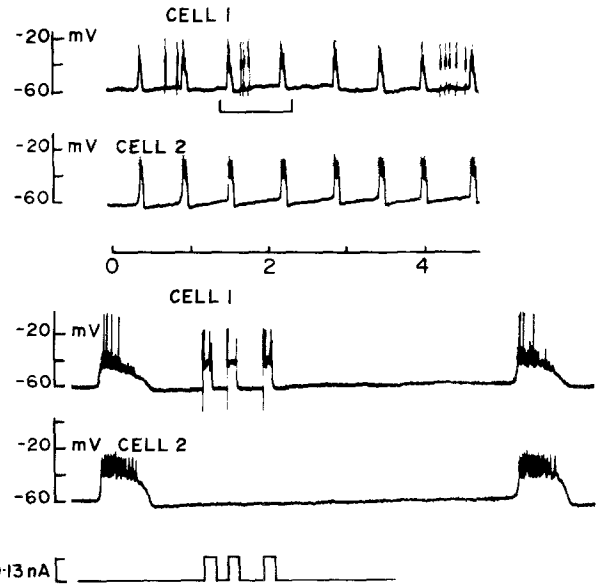

Fig. 1. Synchrony in the glucose-induced bursts in the absence of measurable electrical coupling. Microelectrode tip separation estimated as 35 μm. The upper part shows two segments of the membrane potential records taken after 23 min of exposure to 11 mM glucose. The lower part shows the segments indicated in the upper part at an expanded time base. 0.13 nA current pulses were applied as indicated below the records

time and lasted for the same length of time (i.e., they were synchronous), the spike activity is different. Furthermore, intracellular injection of 0.13 nA current pulses ellicited action potentials in cell 1 but no responses are apparent in cell 2.

In succeeding experiments the electrode tip separation was reduced until a voltage deflection in cell 2 was observed.

Demonstration of Electrical Coupling Among Islet Cells

The maximum tip separation at which a response V_2 could be detected during the application of intracellular current pulses in cell 1 ranged between 30 and 40 μm.

The results from one experiment with the two microelectrode tips 20 μm apart are illustrated in Fig. 2. It may be seen that current injection into cell 1 induced a change in membrane potential in cell 2 which, when the current pulses were in the depolarizing direction and exceeded threshold, induced a train of action potentials in cell 2.

The results presented in Figs. 1 and 2 taken together indicate that, although the islet cells are coupled, the coupling ratio V_2/V_1 decays through the islet tissue with a space constant of the order of

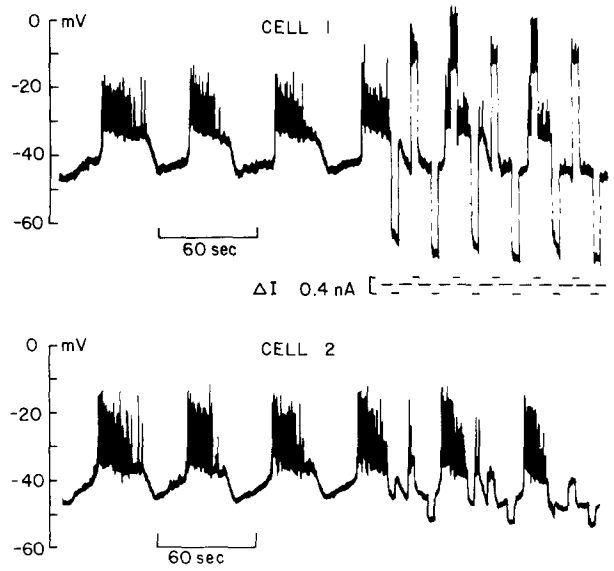

Fig. 2. Demonstration of electrical coupling between neighboring islet cells. Microelectrode tip separation estimated as 20 μm. Burst pattern recorded after 14 min of exposure to 11.1 mM glucose. If the two pulses applied during the bursts in cell 1 are not included, the average values of the responses to the current pulses are: $V_1 = 29.7 \pm 4$ mV; $V_2 = 7.6 \pm 1.9$ mV and $V_2/V_1 = 0.25 \pm 0.04$ (data given as average value ± standard deviation). Note that although the first three bursts are very similar they are not identical. The bursts recorded in cell 1 immediately after impalement were not in synchrony with the bursts in cell 2

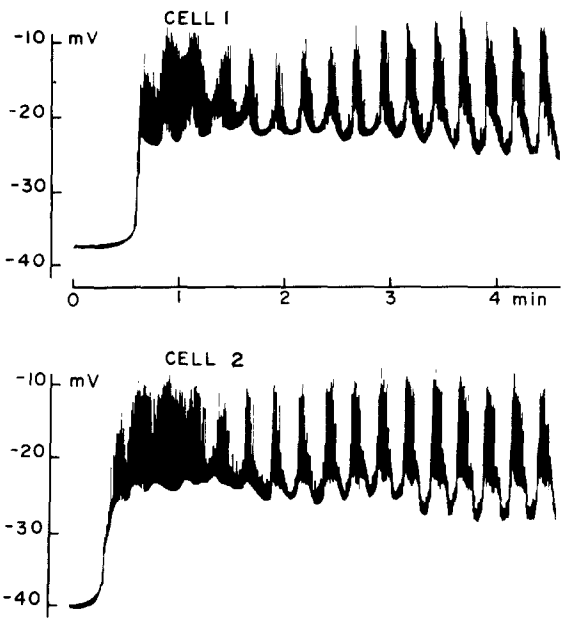

Fig. 3. Onset of glucose-stimulated electrical activity in two distant cells. Microelectrode tips 100 μm apart. The external concentration of glucose was raised from 0 to 11.1 mM 30 sec before the initiation of the electrical activity. Lag time equal to 22 sec

the islet radius. This result does not necessarily imply high junctional resistance between the islet cells as the ratio "resistance of the junctional membrane/resistance of the nonjunctional membrane" determines the value of the space constant of the coupling ratio V_2/V_1 (*see* Discussion).

The Onset of Electrical Activity in Distant and Nearby Cells

Meissner (1976*b*) observed that the bursts recorded in 11.1 mM glucose from two islet cells (separated by distances which were several times the diameter of a β-cell) were in perfect synchrony. This synchrony was maintained in 16.6 mM glucose although the pattern of activity in high glucose was different.

In this section the onset of glucose-induced electrical activity in pairs of cells far apart (Fig. 3) and in pairs of nearby cells (Fig. 4) are compared. Figure 3 shows that the onset of glucose-stimulated electrical activity in two distant cells is completely out of phase. The lag between the start of activity in the first cell and that in the second was 22 sec. Notice that during the first minute the activity is almost continuous and that the burst pattern is obtained 2 to 3 min later (Meissner & Atwater, 1975). When the glucose concentration was raised from zero to 11.1 mM the onset of electrical activity in all cases was asynchronous. In eight experiments the average lag between activity commencing in the first cell and that in the second was 16.6 ± 2.6 sec (data given as mean value ± standard deviation). However, once the steady state had been reached the bursts (*see*, for example, Fig. 1) were in perfect synchrony, even when the separation between the microelectrode tips was several β-cell diameters. The lack of synchrony at the onset of electrical activity shown in Fig. 3 must be due to a reduction in the space constant (as measured by the coupling ratio V_2/V_1) caused by exposure of the islet to KRB without glucose. If the second impalement was made during steady-state conditions (with glucose), the cells are sometimes asynchronous though this phenomenon is transient and may represent nonspecific damage during impalement. When the islets were exposed to 2.8 mM glucose instead of zero glucose, the lag between the activity induced by 11.1 mM commencing in the first cell and that in the second, several β-cell diameters apart, was reduced to 4 ± 0.9 sec.

In all experiments in which the impaled cells were less than 35 μm apart, the onset of glucose-induced (0 to 11.1 mM) activity was always in close synchrony, as shown in Fig. 4. Notice that 0.13 nA

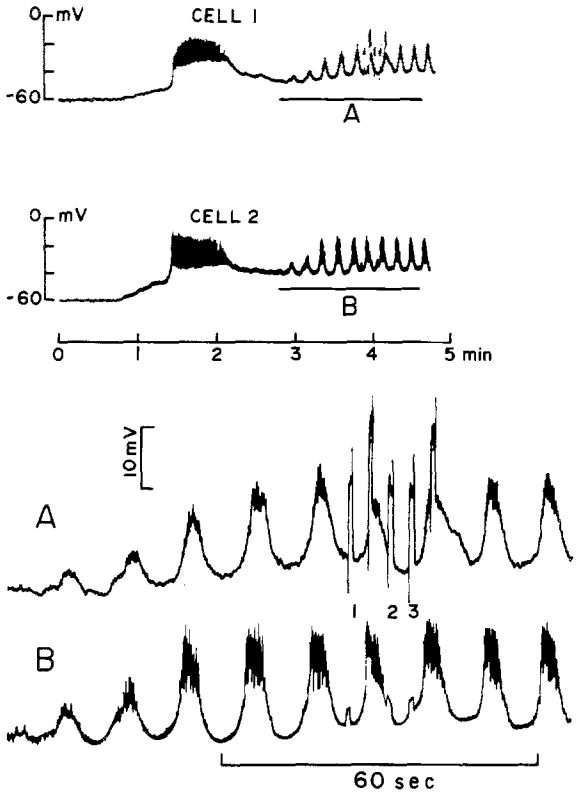

Fig. 4. Onset of glucose-simulated activity in two neighboring cells. Microelectrode tip separation estimated as 30 μm. Glucose was increased from 0 to 11.1 mM at the start of the records shown in the upper part. The segments of the records indicated by the horizontal line have been expanded in the lower part

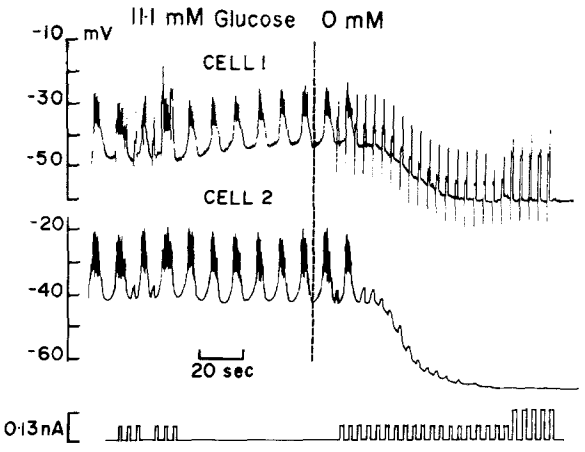

Fig. 5. Changes in V_1 and V_2 after the removal of glucose. Microelectrode tip separation estimated as 10 μm. R_A decreased from $135 \times 10^6\ \Omega$ (measured in the first silent phase after the removal of the glucose) to $80 \times 10^6\ \Omega$ (measured just before increasing the size of the current pulses from 0.065 to 0.13 nA

current pulses produced measurable responses in cell 2. For pulses 1, 2 and 3 indicated in Fig. 4 the calculated coupling ratios are 0.22, 0.17 and 0.19, respectively. Though similar, the two traces are not identical. This is also true of the traces in Fig. 2. Had the pairs of electrodes been in the same cell, they should have differed only in the extent by which they filter the signal.

Changes in Coupling Ratio Induced by Lowering External Glucose

Figure 5 shows the changes in membrane potential of a pair of neighboring cells (microelectrode tips 10 μm apart) induced by lowering glucose from 11.1 mM to zero. It may be seen that the responses V_1 and V_2 to 0.065 nA current pulses start decreasing after the removal of glucose, V_2 becoming too small to measure after the 14th pulse. The implications of this result can be fully realized if one considers the expression for the input resistance proposed (in a slightly different form) by Atwater et al. (1978), i.e.

$$R_A = (R_m + R_j)/((1 + k) + R_j/R_m) \quad (1)$$

where R_m represents the membrane resistance of each cell in the aggregate of coupled cells (assumed to be the same for the k cells in the aggregate) and R_j represents the intercellular resistance between adjacent cells (also assumed to be the same for all the coupled cells). The input resistance R_A can be estimated directly as

$$R_A = V_1/i \quad (2)$$

where i is the size of the injected current. R_A in Fig. 5 decreases from 135×10^6 to $80 \times 10^6\ \Omega$ after the switch to zero glucose. These R_A values fall in the range measured before (Atwater et al., 1978) which indicates that cell 1 is responding to the removal of glucose as described previously.

From Eq. (1) it is clear that it is, in principle, possible to account for a measured change in R_A by assuming either a change in R_j with R_m constant or a change in R_m at constant R_j or a change in both. The additional measurement of V_2 permits a measure of R_j to be made, namely the interelectrode resistance R_e. The relation between R_e and R_j is discussed in the Discussion.

An analysis of the experiment in Fig. 5 in terms of the coupling ratio V_2/V_1 and the parameter R_e is presented in Fig. 6.

The coupling ratio decreases from 0.71 measured with the first pulse to 0.1 measured with the 10th pulse (Fig. 6, upper part). The rapid drop in V_2/V_1 could be explained by a substantial increase in the effective interelectrode resistance R_e (Fig. 6,

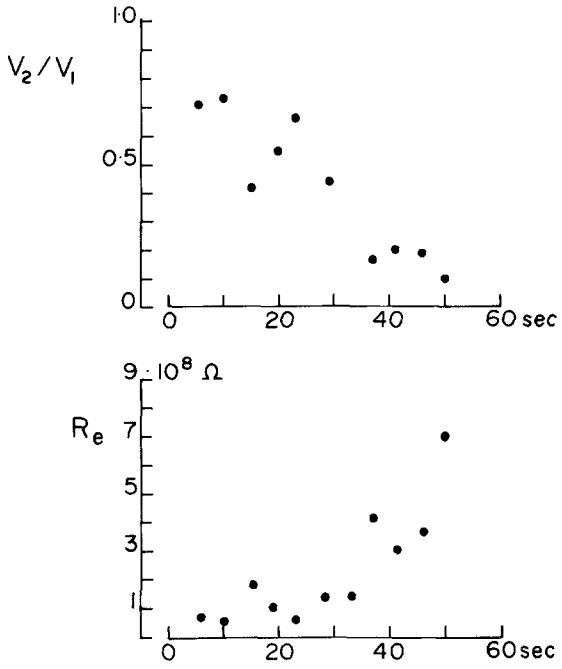

Fig. 6. Effects of glucose removal on coupling ratio and equivalent interelectrode resistance. Data from the experiment illustrated in Fig. 5. *See* Discussion

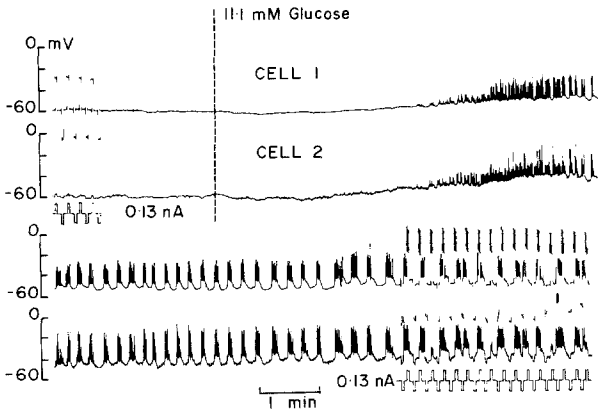

Fig. 7. Effects of 11 mM glucose on coupling. Microelectrodes 35 μm apart. Glucose at 11.1 mM was introduced in the chamber 2 min before the beginning of the record

lower part); it should be emphasized that in the absence of glucose V_2 was too small to be measured. Similar results were obtained in five cell pairs from four different islets.

Changes in Coupling Ratio Induced by Increasing the External Glucose

Figure 7 shows the results of the converse experiment, namely, the elevation of glucose from zero to 11.1 mM. It may be seen that applying 0.13 nA current pulses in the presence of glucose caused small but measurable responses in cell 2 (coupling ratio 0.06). In 11.1 mM glucose the coupling ratio V_2/V_1 increased to 0.14. Derived parameter R_e changed from 4.4×10^9 to 1.9×10^9 Ω.

This experiment was repeated using cell pairs which gave coupling ratios in the range from 0.1 to 0.7 in 11.1 mM glucose. V_2/V_1 always increased and R_e always decreased when the external glucose was raised.

Coupling after Calcium Entry During the Bursts

Electrical activity in islet β-cells involves the activation of voltage-sensitive calcium and potassium channels (Atwater et al., 1979*b*, Ribalet & Beigelman, 1980). It is proposed that in the absence of glucose the level of intracellular free ionized calcium is raised due to reduced buffering. This leads to activation of the calcium-gated potassium permeability ($P_{K-Ca^{2+}}$) which hyperpolarizes the cells too close to the K^+ equilibrium potential. Upon addition of glucose the intracellular calcium is reduced (Hellman, Honkanen & Gylfe, 1982). This reduces the $P_{K-Ca^{2+}}$ leading to depolarization and voltage-sensitive Ca^{2+} channel activity. This in turn raises the intracellular calcium level which activates $P_{K-Ca^{2+}}$ bringing the burst to a finish (Atwater, Dawson, Eddlestone & Rojas, 1980).

The significant feature of this proposed model from the viewpoint of intercellular communication is the implication of an oscillatory intracellular Ca^{2+}. If this was the case, it may be expected that the coupling between cells in the islet might change during the burst pattern.

To test this idea current pulses were applied during the long-lasting silent phases seen in a typical biphasic electrical response to a sudden increase in glucose (Meissner & Atwater, 1975). The results from one experiment of this type are illustrated in Figs. 8 and 9.

V_1 and V_2 were measured as a function of time from the end of a burst of electrical activity. From these measurements V_2/V_1 and R_e were calculated (*see* Discussion).

The results presented in Fig. 8*B* clearly indicate that the coupling ratio V_2/V_1 remains nearly constant during the 112 sec after calcium entry caused by action potentials during the bursts. The equivalent interelectrode resistance R_e shown in Fig. 9 hints at a tendency to decrease though the scatter is large. Similar results were obtained in two further experiments.

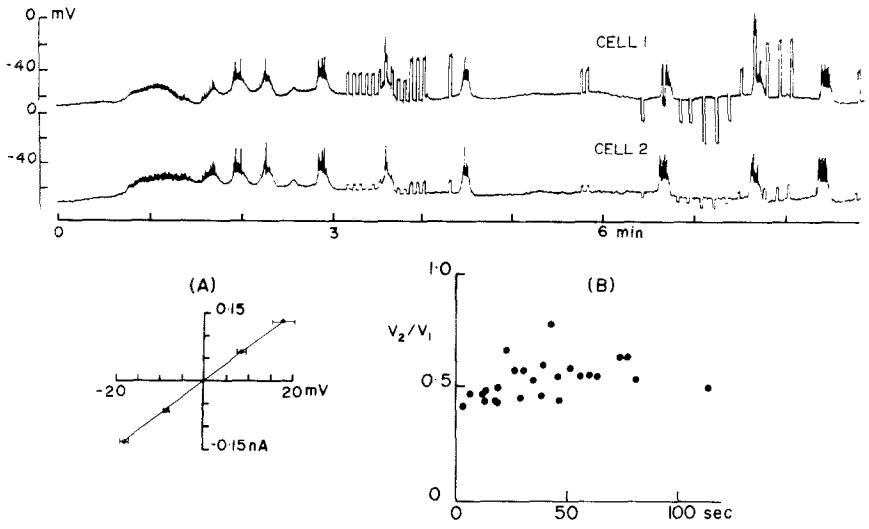

Fig. 8. Coupling ratio along the silent phase after a burst. Microelectrodes 18 μm apart. At the start of the records glucose was increased from 0 to 11.1 mM. (*A*) Current injected as a function of V_1. Note that these values were corrected to take into account an increase in microelectrode resistance from 150×10^6 to 300×10^6 Ω. Each point represents the average value and the horizontal bars ± SD. (*B*) V_2/V_1 as a function of time after the termination of the burst immediately before the pulse. The abortive response after the 3rd minute was not considered as a burst

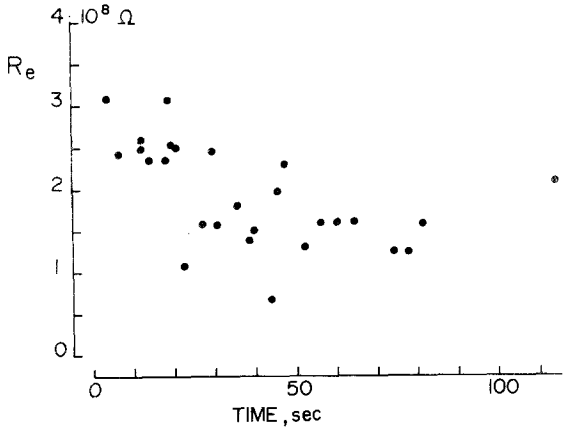

Fig. 9. Changes in equivalent interelectrode resistance after calcium entry. R_e values as a function of time. Data from Fig. 8. For calculation of R_e *see* Discussion

Table 2. Effects on the coupling ratio V_2/V_1 of varying glucose

Glucose concentration (mM)	V_2/V_1 (Mean ± SD)	Number of cell pairs
0	0.27 ± 0.13	21
5.6	0.32 ± 0.13	7
11.1	0.58 ± 0.31	37
16.7	0.72 ± 0.33	14
22.2	0.78 ± 0.27	6

At 11.1 and 16.7 mM glucose measurements were made at the mid-point of the silent phases between the bursts. For these experiments the estimated microelectrode tip separation ranged from 10 to 35 μm. In all cell pairs several glucose concentrations were used.

Effects of Glucose on Coupling in Steady-State Conditions

Eighty-five β-cell pairs were examined to determine the glucose dependence of the coupling ratio in steady-state conditions. The results from these experiments are summarized in Table 2 and in Fig. 10.

The interelectrode distance for these experiments ranged from 10 to 35 μm. For those experiments which gave bursts of electrical activity, V_1 and V_2 were measured using hyperpolarizing pulses applied during the silent phase between the bursts. The data in Table 2 show that the coupling ratio increases as the glucose concentration in the external medium increases throughout the physiological range.

Three experiments from Table 2 were selected to prepare Fig. 10. For these cell pairs more than one glucose concentration had been applied and the interelectrode distance was kept in the range from 15 to 25 μm. Fig. 10*A* shows that, in steady-state conditions, the coupling ratio increases with the concentration of glucose in the Krebs solution. The corresponding changes in the parameter R_e are shown in Fig. 10*B*. It may be seen that the equivalent interelectrode resistance decreases as the concentration of glucose is increased.

If intracellular Ca^{2+} is maintained at low levels by energy-dependent sequestration and/or extrusion of the cation, reduction of ATP should lead to a rise in this calcium. As in the absence of glucose the β-cell ATP decreases (Ashcroft, Weerasinghe &

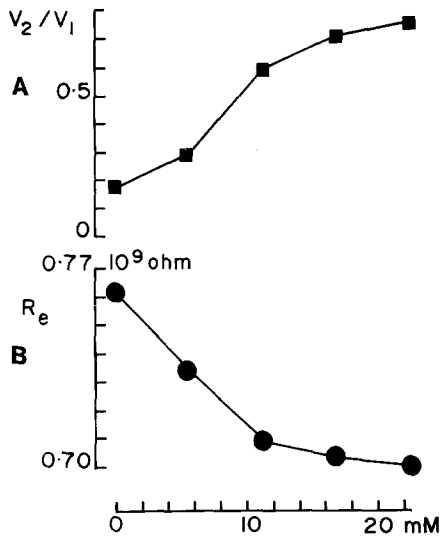

Fig. 10. Effects of glucose on cell-to-cell coupling. *A*. Average coupling ratio as a function of glucose concentration in steady-state conditions (three experiments). *B*. Average value of the equivalent interelectrode resistance calculated with the V_1 and V_2 values for the experiments in part *A* (*see* Discussion)

Randle, 1973), the simplest interpretation of the experiments in Table 2 and Fig. 10 is that the decreased coupling ratio measured in the absence of glucose is due to an increase in cytosolic Ca^{2+} which in turn should increase R_j and therefore R_e (Simpson, Rose & Loewenstein, 1977; Rose & Rick, 1978).

Effects of Membrane Potential on Coupling Ratio

Two different series of experiments were carried out to determine the effects of membrane potential on V_2/V_1. In these experiments pairs of cells were impaled in the presence of 11.1 mM glucose and rectangular pulses of current were injected to confirm the existence of intercellular communication between the two cells. The glucose concentration was then decreased to a nonstimulatory level, usually around 5 mM at which the coupling ratio decreased but remained significant.

In the first group of experiments rectangular current pulses of different magnitudes were applied to cell 1 with alternating polarity in order to generate current-voltage plots for both cells 1 and 2. The roles of the electrodes were then exchanged so that the current was injected into the other impaled cell and the pulse program was repeated. This, in all, generated four current-voltage plots: Cell A injected, $i - V_1$ and $i - V_2$; Cell B injected, $i - V_1$ and $i - V_2$.

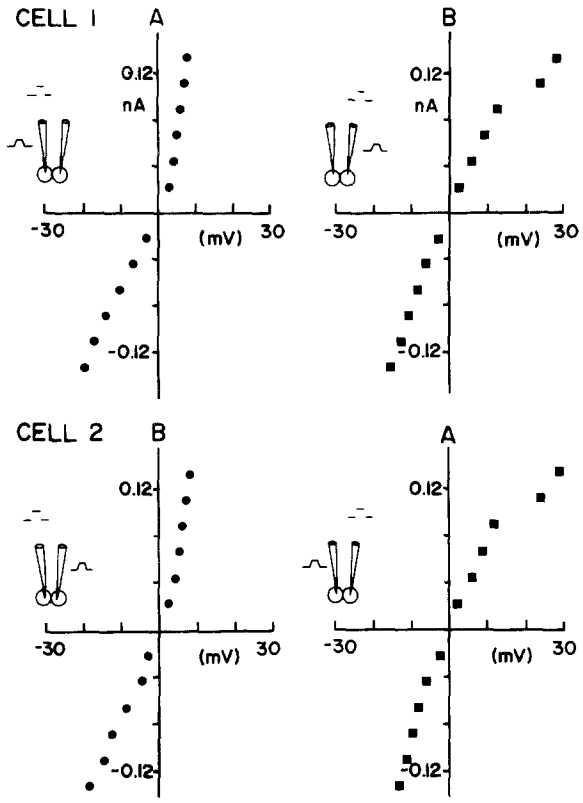

Fig. 11. Current-voltage relationships for two adjacent cells. Upper part represents the $i - V$ curves for cells A_1 and B_1. Lower part represents the $i - V$ curves for cells A_2 and B_2. Input resistances from the slope of the $i - V$ curves in the negative quadrangle as follows: Cell A = 134 × 10^6 Ω; Cell B = 105 × 10^6 Ω. 5 mM glucose was present throughout the experiment

By comparison of the upper and lower graphs in each cell A or B in Fig. 11, it may be seen that the voltage deflection in cell 2 was almost identical to that in cell 1 throughout the current pulse range utilized, indicating that the coupling ratio, which was close to unity, did not change with induced displacements in membrane potential during the pulses. Similar results were obtained in four additional experiments in 5 mM glucose with coupling ratios between 0.2 and 0.75 which remained constant throughout the membrane potential range examined. The data suggest that the communication pathway between the islet cells is insensitive to induced displacements of membrane potential in the range from 3 to 20 mV.

Considering the $i - V_1$ plots (upper part) it is immediately obvious that the current-voltage relationships are dissimilar. Cell A (on the left side) appears to exhibit a slight outward-going, or normal, rectification. Cell B shows a deviation from linearity of the current-voltage relationship with outward-going current pulses in excess of 0.088 nA.

A further increase in the size of the current pulses induced action potentials. V_1 and V_2 measurements in the presence of spikes are difficult to interpret and for this reason this part of the $i - V_1$ curve will not be considered.

In the second group of experiments, the effects of membrane potential on the coupling ratio over a wider range of potentials were studied. The external potassium concentration was augmented three consecutive times, from 3.5 to 28 mM, from 3.5 to 56 mM and from 3.5 to 14 mM (as illustrated in Fig. 12) while maintaining the glucose concentration constant at 5 mM. The K^+ and Na^+ concentrations were varied such that three pulses of increased K^+ could be applied, the Na^+ being decreased to maintain constant osmotic pressure. As the P_K/P_{Na} ratio is large in the β-cell, the steady-state membrane potential followed the changes predicted from the Goldman-Hodgkin-Kätz equation (Atwater et al., 1978).

When perifusing with raised K^+ rectangular current pulses were injected into cell 1 and the coupling ratio calculated. V_2/V_1 values at the three membrane potentials are given in Fig. 12. It may be seen that changes in membrane potential of up to 55 mV do not appear to influence the coupling between the cells, indicating that the communication pathway is not influenced by the membrane potential.

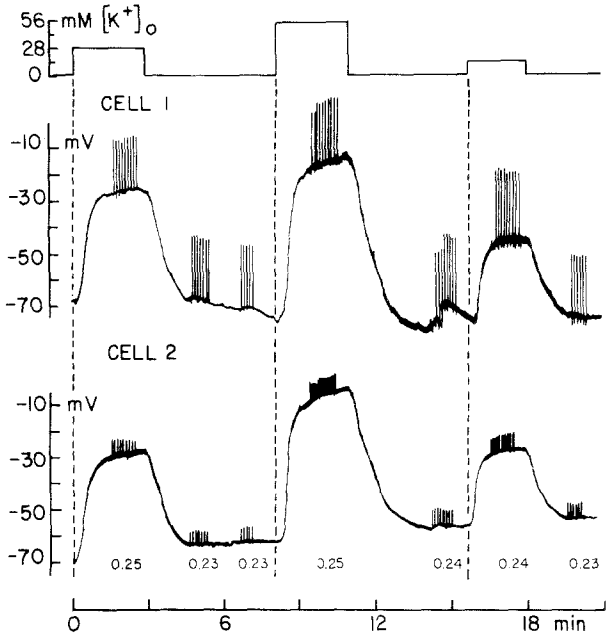

Fig. 12. Effect of membrane potential changes induced by an elevation of the external potassium on the coupling between adjacent cells. Three potassium concentrations were applied: 28, 56 and 14 mM (indicated by the vertical dotted lines). Current pulses of 0.13 nA were injected. Numbers under the panel indicate the coupling ratio calculated from the last 4 current pulses

Effects of Mitochondrial Blockers on Coupling Ratio

Inhibition of ATP production by electron transfer chain blockers and uncouplers of phosphorylation from respiration should produce the same results as removing glucose (*see* Fig. 5). Electron transfer inhibitors and uncouplers have all been shown to cause an increase in the level of Ca^{2+} in the protoplasm (Rojas & Hidalgo, 1968) and a 10 to 20 mV hyperpolarization associated with a 30% reduction in R_A of the glucose-stimulated β-cell (Atwater et al., 1979*b*). Their effects were interpreted in terms of ATP depletion and consequent elevation of Ca^{2+} in the protoplasm, this interpretation being supported by the results of Sugden and Ashcroft (1978) who showed that uncouplers greatly reduced $^{45}Ca^{2+}$ uptake into isolated islet mitochondria.

In these experiments two cells were impaled in the presence of 11.1 mM glucose and rectangular current pulses injected into cell 1 to check that a clear V_2 response could be measured. Having established this, the system was treated to reduce the available ATP and thus raise Ca^{2+}. If the two resistances R_m and R_j were changed at significantly different levels of Ca^{2+}, or at different rates, it would be possible to detect changes in the coupling ratio independent of the changes in R_A.

The results of one such experiment are presented in Fig. 13. Nine sec after the removal of glucose the input resistance V_1/i decreased from 153 $\times 10^6$ to 116 $\times 10^6$ Ω in 10 sec and the coupling ratio V_2/V_1 showed a slight decrease from 0.9 to 0.85 (*also see* Fig. 5). The equivalent resistance R_e increased from 30.6 $\times 10^6$ to 39.6 $\times 10^6$ Ω as a result of removing glucose.

The addition of 1 μM FCCP (carbonyl-cyanide, *p*-tri-fluoromethoxyohenylhydrazone) in the absence of glucose causes no significant changes in the input resistance (●) or in the coupling ratio (■). To monitor reversibility, current pulses were applied during subsequent re-addition of glucose. The input resistance and the coupling ratio returned to their control values.

The effects of FCCP were further examined in the presence of 11.1 mM glucose. The results of one experiment of this type are presented in Fig. 14.

As observed before (Atwater et al., 1979*b*) FCCP caused a cessation of the electrical activity and the membrane hyperpolarized to the potential level measured in the absence of glucose in both

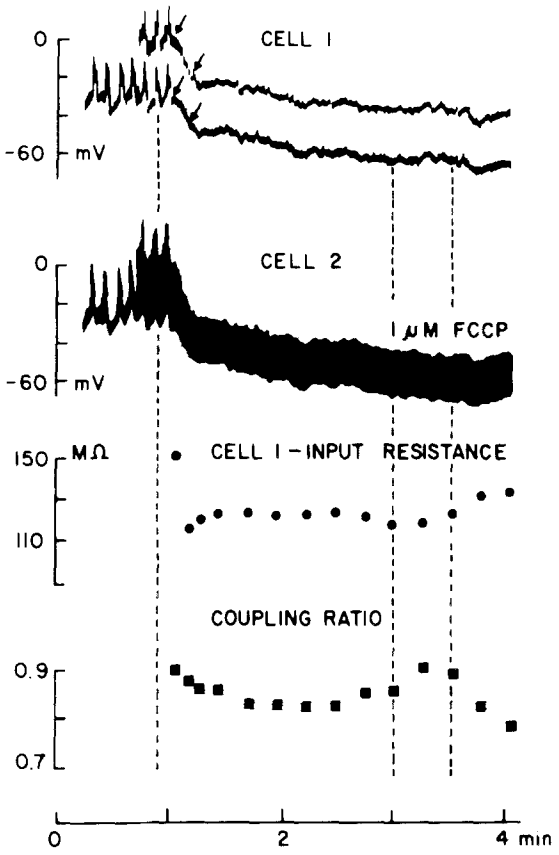

Fig. 13. Effects of FCCP in the absence of glucose on input resistance and coupling ratio. Microelectrode tip separation estimated as 10 μm. From top to bottom: Membrane potential records for cells 1 and 2, input resistance and coupling ratio. The three vertical dotted lines indicate the removal of glucose, and the addition and removal of 1 μM FCCP. The following values were measured at the times indicated by the arrows injecting 0.22 nA of current: $V_2/V_1 = 0.9$ and 0.85. $R_e = (V_1 + V_2)(V_1 - V_2)/iV_2$ increased from 30.6×10^6 to 39.6×10^6 Ω

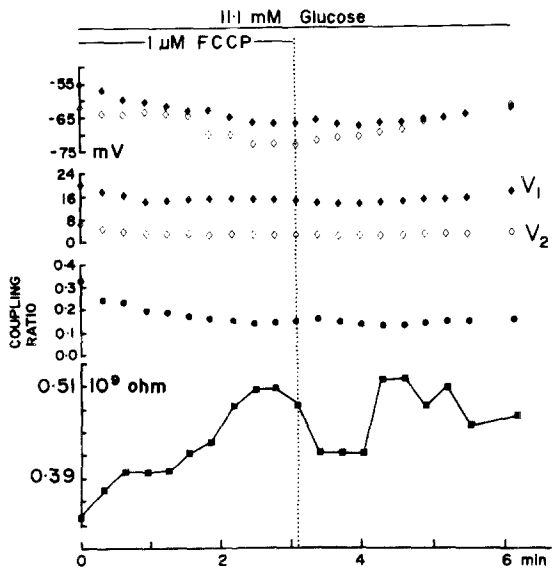

Fig. 14. Effects of FCCP in the presence of glucose upon intercellular coupling. From top to bottom: Membrane potential of cell 1 and cell 2; current pulse-induced voltage deflection in cell 1 (♦) and cell 2 (◇); coupling ratio (●) and R_e (■). The dotted vertical line indicates the removal of 1 μM FCCP and the return to 11.1 mM glucose alone. $i = 0.18$ nA

cells. This hyperpolarization was accompanied by a decrease in R_A shown by a reduction in the size of V_1 in response to constant current pulses. The coupling ratio (●) also decreased from 0.33 before to 0.15 3 min after adding 1 μM FCCP. The lower graph illustrates the possible change in the interelectrode resistance R_e. It may be seen that R_e increases from 0.3×10^9 to 0.5×10^9 Ω during the exposure to FCCP. After the removal of the FCCP the input resistance began to increase from 67.5×10^6 Ω (measured immediately after) to 92.5×10^6 Ω (measured 3.4 min after). This 37% increase in input resistance was accompanied by a marginal increase in coupling ratio. In this experiment the coupling ratio reached its control level 15 min following the end of the record shown in Fig. 14.

Effects of Mitochondrial Blockers on Coupling with the Calcium-Activated Potassium Channel and Calcium Channel Blocked

We have seen that experiments in which a removal of energy (which may be reflected by a rise of cytosolic calcium), by removing glucose or by adding mitochondrial blockers, always reduces R_A (*see* Figs. 5, 13 and 14; *also see* Table 1 in Atwater et al., 1978).

To determine whether or not mitochondrial blockers affect the derived parameter R_e the ionic channels in the nonjunctional membrane are blocked with specific agents.

To minimize the shunting effects caused by stimulation of the potassium calcium-gated channel, quinine may be used (Atwater et al., 1979*b*). The effects of quinine on β-cell electrical activity are not reversible and there is a progressive decay of electrical activity. For this reason it was considered prudent to restrict observations in the presence of quinine to the first 10 min after a regular pattern of spikes was established.

In the experiment summarized in Fig. 15, 0.1 μM FCCP was added 1.5 min after the constant spike activity, characteristic of quinine stimulation, had been established (Atwater et al., 1979*b*). After 2

min the FCCP concentration was raised to 0.25 μM and 2 min after this the concentration was raised to 1 μM. It may be seen that in the presence of quinine the $P_{K-Ca^{2+}}$ was blocked as FCCP caused no decrease in R_A nor any perceptible hyperpolarization in the two cells (compare this description with the results in Fig. 14). Under these conditions, any changes in R_e caused by FCCP should be readily discernible. The temporal course of R_e calculated from V_1 and V_2 values is shown in the lower part of Fig. 15. It may be seen that, although the scatter of the points is large, R_e increases from an average value of 0.7×10^9 Ω in 0.1 μM FCCP to 0.8×10^9 Ω in 1.0 μM FCCP. The large variation in the R_e values is caused by inaccurate V_1 and V_2 measurements in the presence of continuous spike activity induced by quinine.

It is possible to block action potentials recorded in the presence of quinine using Co^{2+} (Atwater et al., 1981). In a further attempt to measure any possible changes in R_e induced by a different mitochondrial blocker with R_m at maximum and constant value, three experiments were carried out in which $P_{K-Ca^{2+}}$ was blocked with 200 μM quinine, P_{Ca} was blocked with 2 mM Co^{2+}, and the uncoupler 2,4 dinitrophenol (DNP) was used to elevate intracellular Ca^{2+}.

The results from one of these experiments can be summarized as follows. The control value for the coupling ratio was 0.22 and the derived parameter R_e was $(0.50 \pm 0.15) \times 10^9$ Ω. Four min after the addition of 200 μM quinine R_e increased to $(2.4 \pm 0.1) \times 10^9$ Ω. Five min after the application of 0.2 mM DNP R_e further increased to $(25.0 \pm 4.5) \times 10^9$ Ω. However, 2 min after removing DNP this derived parameter had reduced again to $(1.6 \pm 0.4) \times 10^9$ Ω. Although the other two experiments gave similar results, the changes in R_e induced by quinine and DNP were less accentuated.

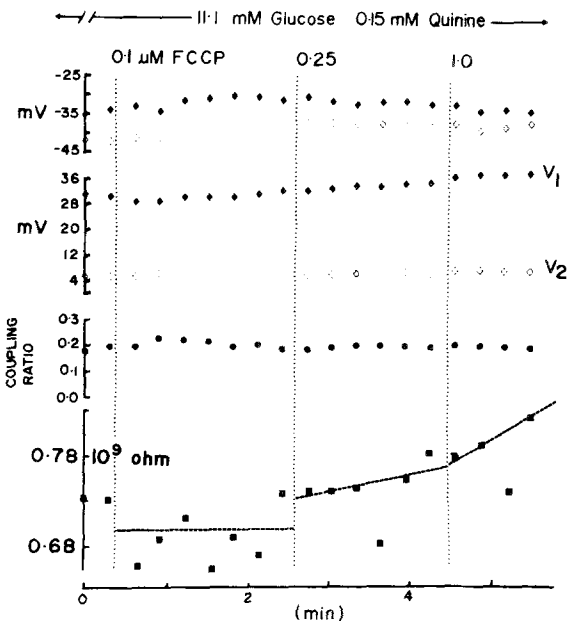

Fig. 15. Effects of FCCP on cell-to-cell coupling in the presence of quinine. Symbols as follows: (♦): Membrane potential of cell 1; (♦): V_1; (◇): Membrane potential of cell 2; (◇): V_2; (●): Coupling ratio; (■): R_e. Lines drawn through the R_e points were fitted by eye

Discussion

Pancreatic Islet Cells are Electrically Coupled

The most important result of this work is the demonstration of electrical coupling between excitable cells in the islet of Langerhans from mouse.

With glucose present and under steady-state conditions, injecting current into cell 1 measurably displaced the membrane potential of a second cell 2, provided the microelectrodes were less than 35 μm apart. In other words, there is an electrotonic spread of current between electrically active islet cells. Since only electrically active cells were used it is possible that only β-cells were studied.

Under steady-state conditions, glucose facilitates electrical coupling. The time course of this effect of glucose could be followed by measuring the coupling ratio after the removal of glucose from the external medium. A rapid decrease in V_2/V_1 was observed (Figs. 5 and 6). Upon re-addition of glucose (Fig. 7) the coupling ratio returned to the control value.

The results from two different experiments indicate that the current through the intercellular junctions in an islet of Langerhans is not rectified. Firstly, the current-voltage relationships are similar in both cells and remain similar when the role of the microelectrodes is changed. Secondly, when both impaled cells are depolarized by increasing the external potassium, the coupling ratio remains unchanged. These results suggest that the membrane potential of the islet cells *per se* does not affect the intercellular channel. The electrical properties of the intercellular pathway studied in this work are similar to those of the junction described by Loewenstein and Kanno (1964) and when considered with the available morphological evidence (Orci, 1974; Meda, Amherdt, Perrelet & Orci, 1979;

Meda et al., 1980*a*,*b*,*c*) are consistent with the view that intercellular communication is mediated via gap junctions.

Interelectrode Resistance as a Measure of Junctional Resistance

The simplest circuit relating the three electrical parameters measured, i, V_1 and V_2, comprises three resistors. The resistances between each measuring point (at which V_1 and V_2 are monitored) and ground which, since the two impaled cells are indistinguishable, must have identical value and, which carry currents i_1 and i_2, respectively. The third resistor connects the two measuring points and is the interelectrode resistance R_e. Using the relations

$$i = i_1 + i_2$$
$$i_1 = V_1/R$$
$$i_2 = V_2/R$$

and

$$R_e = (V_1 - V_2)/i_2$$

the following expression for R_e can be derived:

$$R_e = (V_1 + V_2)(V_1 - V_2)/(iV_2). \quad (3)$$

R_e values calculated using this equation are given in the text and in the Figures. In the next section a relationship between R_e and the true junctional resistance will be discussed.

Values for the Junctional and Nonjunctional Membrane Resistances and for the Space Constant

The current injected into one of the two impaled cells can be assumed to flow radially from the injected cell into a sphere of islet tissue surrounding the electrode through which current was injected.

When describing the spread of current from a localized source within the islet tissue it is useful to assume that increments of membrane area are directly proportional to $r^2\delta r$ where r is the distance from the point source and δr represents an increment in radial distance. As the individual cells in the islet are small and relatively uniform in size, the total membrane area per unit volume will be approximately constant. In order to calculate the junctional and nonjunctional membrane resistances it is necessary to estimate the surface area-to-volume ratio for the islet tissue.

The average mouse islet volume is 2.5×10^{-5} cm^3 (Scott, Atwater & Rojas, 1981). Assuming that 64% of this volume represents endocrine cells and taking the cell volume as 0.9×10^{-9} cm^3 (the volume of a sphere of radius 6×10^{-4} cm; Dean, 1973), there would be 1.78×10^4 cells per islet with a total surface area of 8×10^{-2} cm^2. Then, the surface area-to-volume ratio (χ) for the islet tissue is estimated as 5×10^3 cm^{-1}.

With these simplifying assumptions a relation between the voltage measured at a point r_2 cm from the point of current injection, the injected current i, the specific membrane resistance R_m (Ωcm^2), the specific intracellular resistivity R_i (Ωcm), and the surface-to-volume ratio for the islet tissue χ (cm^{-1}) has been obtained (Jack, Noble & Tsien, 1975), namely,

$$\lambda^2[\delta^2 V_2/\delta r_2^2 + 2/r_2(\delta V_2/\delta r_2)] - (\tau_m \delta V_2/\delta t + V_2) = 0 \quad (4)$$

where

$$\lambda = (R_m/(\chi R_i))^{1/2} \quad (5)$$

represents the space constant in cm and τ_m is the membrane time constant ($=R_m \times C_m$). If

$$\delta V/\delta t = 0$$

then the solution to the differential equation is

$$V_2 = ((iR_i)/(4\pi r))e^{-r/\lambda} \quad (6)$$

(*see* Jack et al., 1975). Note that for $r = 0$ there is a singular point resulting from the infinite current density at a point source.

Figure 16 shows how V_2/i varies with estimated interelectrode distance in a number of experiments (in which the injected current i varied). Values of R_i and R_m were chosen such as to minimize the sum of the squares of residuals on the ordinate and the resulting best-fit curve is shown which corresponds to $R_i = 1.5 \times 10^6$ Ωcm and $R_m = 0.64 \times 10^6$ Ωcm^2. The quality of fit is rather insensitive to the latter parameter which is not, therefore, well determined. The resistance of the junctional membrane R_j equals χR_i and is 7.7×10^9 Ω. These values give a space constant (λ) of 90.9 μm. It should be mentioned here that, for values of r_2 near 20 μm, an e-fold decrease in V_2 occurs when r_2 is increased by between 20 and 30 μm. If, as in the case of a linear conductor (Jack et al., 1975), V_2 decays exponentially with r_2 this increment in r_2 represents the space constant. However, in the case of a volume conductor as discussed above the space constant is calculated using Eq. (6).

Relationship Between Interelectrode Resistance and Junctional Membrane Resistance

The interelectrode resistance is approximately proportional to R_i in the range from 0.1 to 10 × R_i and to R_m in the range from 0.1 to 10 × R_m. This can be verified by assuming that V_1 is a measure of the voltage 5 μm from the center of the sphere (were it at the center the voltage would be infinite due to an infinite current density); then Eq. (6) can be used to compute values of V_1 and V_2 (at 20 μm) for various values of R_i and R_m from which the equivalent R_e can be calculated. The interelectrode resistance was used as a measure of R_i and therefore of R_j throughout most of the study.

Note that the model assumes that the extracellular resistance between each impaled cell and ground is negligible compared to R_A. The evidence supporting this notion depends on the observation that a microelectrode shows no change in resistance as it passes through an islet unless it actually impales a cell. Furthermore, insulin secreted from a β-cell is able to leave an islet and this implies that a porous route must exist from each β-cell to the outside of the tissue.

Implications of the Results

Several conclusions can be drawn from the results which do not depend on how the cells are geometrically arranged. First there are electrically coupled cells within the surface layers of the islet. This may include several cell types but, since only electrically active cells were studied and, because electrical activity (bursts) are glucose dependent in a way that is related to insulin secretion (Scott, Atwater & Rojas, 1981), we propose that the cell coupling studied here represents β-cell to β-cell electrical coupling. The coupling in 11.1 mM glucose allows an injected signal to be propagated over about 35 μm. Glucose which fuels β-cells increases the degree of coupling, while uncouplers which de-energize the system reduce the degree of coupling. This is consistent with the view that the intracellular calcium concentration is normally at a level which can control insulin secretion and intercellular coupling. The data is too scattered to allow changes in intercellular coupling to be detected during the silent phase (between bursts).

Within the framework of the model it has been shown that variations in the intercellular coupling due to alterations in the fuel supply can, to a large extent, be attributed to changes in the intercellular resistance.

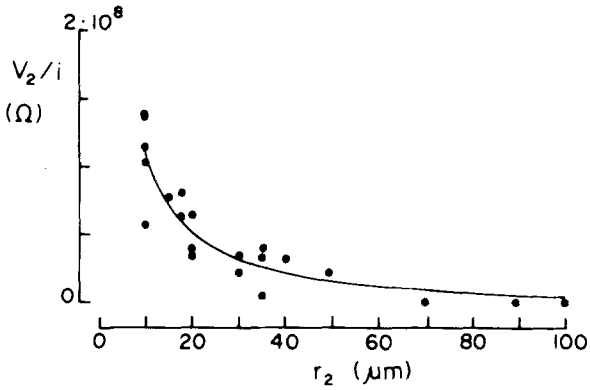

Fig. 16. Space constant for cell-to-cell coupling in the islet tissue. Data from 23 experiments. As the size of the current injected varied from 0.065 to 0.22 nA the vertical axis has been normalized to represent V_2/i. All experiments under steady-state 11.1 mM glucose stimulation. The curve represents a least-squares regression fit of Eq. (6) given in the text to the experimental points. Computation started at r = 10 μm. For values of the parameters obtained from the fit *see* Discussion

The authors are pleased to thank Dr. Illani Atwater for many stimulating discussions and suggestions during the course of this work. This research was supported by grants from the Wellcome Trust, the British Diabetic Association and the Medical Research Council.

References

Ashcroft, S.J.H., Weerasinghe, L.C.C., Randle, P.J. 1973. Interelationship of islet metabolism, adenosine triphosphate content and insulin release. *Biochem. J.* **132:**223–231

Atwater, I., Dawson, C.M., Eddlestone, G.T., Rojas, E. 1981. Voltage noise measurements across the pancreatic β-cell membrane: Calcium channel characteristics. *J. Physiol. (London)* **314:**195–212

Atwater, I., Dawson, C.M., Ribalet, B., Rojas, E. 1979*a*. Potassium permeability activated by intracellular calcium ion concentration in the pancreatic β-cell. *J. Physiol. (London)* **288:**575–588

Atwater, I., Dawson, C.M., Scott, A., Eddlestone, G.T., Rojas, E. 1980. The nature of the oscillatory behaviour in electrical activity from pancreatic β-cell. *Horm. Metab. Res. Suppl.* **10:**100–107

Atwater, I., Ribalet, B., Rojas, E. 1978. Cyclic changes in potential and resistance of the β-cell membrane induced by glucose in islets of Langerhans from mouse. *J. Physiol. (London)* **278:**117–139

Atwater, I., Ribalet, B., Rojas, E. 1979*b*. Mouse pancreatic β-cells: Tetraethylammonium blockage of the potassium permeability increase induced by depolarization. *J. Physiol. (London)* **288:**561–574

Dean, P.M. 1973. Ultrastructural morphomotry of the pancreatic β-cell. *Diabetologia* **9:**115–119

Dean, P.M., Matthews, E.K. 1968. Electrical activity in pancreatic islet cells. *Nature (London)* **219:**389–390

Dean, P.M., Matthews, E.K. 1970*a*. Glucose induced electrical

activity in pancreatic islet cells. *J. Physiol.* (*London*) **210:**255–264

Dean, P.M., Matthews, E.K. 1970*b*. Electrical activity in pancreatic islet cells: Effects of ions. *J. Physiol.* (*London*) **210:**265–275

Eddlestone, G.T., Rojas, E. 1980. Evidence of electrical coupling between mouse pancreatic B-cells. *J. Physiol.* (*London*) **303:**76–77P

Hellman, B., Honkanen, T., Gylfe, E. 1982. Glucose inhibits insulin release induced by Na^+ mobilization of intracellular calcium. *FEBS Lett.* **148:**289–292

Jack, J.J.B., Noble, D., Tsien, R.W. 1975. Electric current flow in excitable cells. Clarendon Press, Oxford

Kohen, E., Kohen, C., Thorell, B., Mintz, D.H., Rabinovitch, A. 1979. Intercellular communication in pancreatic islet monolayer cultures: A microfluorometric study. *Science* **204:**862–865

Loewenstein, W.R. 1981. Junctional intercellular communication: The cell-to-cell membrane. *Physiol. Rev.* **61:**829–913

Loewenstein, W.R., Kanno, Y. 1964. Studies on epithelial (gland) cell junction. I. Modification of surface membrane permeability. *J. Cell Biol.* **22:**565–586

Matthews, E.K., Sakamoto, Y. 1975*a*. Electrical characteristics of pancreatic islet cells. *J. Physiol.* (*London*) **246:**421–437

Matthews, E.K., Sakamoto, Y. 1975*b*. Pancreatic islet cells: Electrogenic and electrodiffusional control of membrane potential. *J. Physiol.* (*London*) **246:**439–457

Meda, P., Amherdt, M., Perrelet, A., Orci, L. 1979. Coupling between insulin-containing cells. A morphological approach. *Int. Cong. Series No. 500, Diabetes*. W.K. Waldausl, editor. Excerpta Medica, North-Holland

Meda, P., Denef, J.F., Perrelet, A., Orci, L. 1980*a*. Nonrandom distribution of gap junctions between pancreatic β-cells. *Am. J. Physiol.* **238:**C114–C119

Meda, P., Halban, P., Perrelet, A., Renold, A.E., Orci, L. 1980*b*. Gap junction development is correlated with insulin content in the pancreatic β-cell. *Science* **209:**1026–1028

Meda, P., Perrelet, A., Orci, L. 1979. Increase of gap junctions between pancreatic β-cells during stimulation of insulin secretion. *J. Cell Biol.* **82:**441–448

Meda, P., Perrelet, A., Orci, L. 1980*c*. Gap junctions and β-cell function. *Horm. Metab. Res. Suppl.* **10:**157–162

Meissner, H.P. 1976*a*. Electrical characteristics of the pancreatic β-cell. *J. Physiol.* (*Paris*) **72:**757–767

Meissner, H.P. 1976*b*. Electrophysiological evidence for coupling between β-cells of pancreatic islets. *Nature* (*London*) **262:**502–504

Meissner, H.P., Atwater, I. 1975. The kinetics of electrical activity of B-cells in response to a square wave stimulation with glucose and libenclamide. *Horm. Metab. Res.* **8:**11–15

Michaels, R.L., Sheridan, J.D. 1981. Islets of Langerhans: Dye coupling among immunocytochemically distinct cell types. *Science* **214:**801–803

Orci, L. 1974. A portrait of the pancreatic β-cell. *Diabetologia* **10:**163–187

Orci, L., Unger, R.H., Renold, A.E. 1973. Structural coupling between pancreatic islet cells. *Experientia* **29:**1015– 1018

Ribalet, B., Beigelman, P.M. 1979. Cyclic variation of K^+ conductance in pancreatic β-cells: Ca^{2+} and voltage dependence. *Am. J. Physiol.* **237:**C137–C146

Ribalet, B., Beigelman, P.M. 1980. Calcium action potentials and potassium permeability activation in pancreatic β-cells. *Am. J. Physiol.* **239:**C124–C133

Rojas, E., Hidalgo, C. 1968. Effect of temperature and metabolic inhibitors on ^{45}Ca outflow from squid giant axons. *Biochim. Biophys. Acta* **163:**550–556

Rose, B., Loewenstein, W.R. 1975. Calcium ion distribution in cytoplasm visualized by aequorin. Distribution in the cytosol is restricted due to energized sequestering. *Science* **190:**1204–1206

Rose, B., Loewenstein, W.R. 1976. Permeability of a cell junction and the local cytoplasmic free ionized calcium concentration: A study with aequorin. *J. Membrane Biol.* **28:**87–119

Rose, B., Rick, R. 1978. Intracellular pH, intracellular free Ca, and permeability of cell junction. *J. Membrane Biol.* **44:**377–415

Rose, B., Simpson, I., Loewenstein, W.R. 1977. Calcium ion produces graded changes in permeability of membrane channels in cell junction. *Nature* (*London*) **267:**625–627

Scott, A.M., Atwater, I., Rojas, E. 1981. A method for the simultaneous measurement of insulin release on β-cell membrane potential in single mouse islets of Langerhans. *Diabetalogia* **21:**470–475

Simpson, I., Rose, B., Loewenstein, W.R. 1977. Size limit of molecules permeating the junctional membrane channels. *Science* **195:**294–296

Sugden, M.C., Ashcroft, S.J.H. 1978. Effects of phosphoenolpyruvate, other glycolytic intermediates and methylxanthines on calcium uptake by a mitochondrial fraction from rat pancreatic islets. *Diabetologia* **15:**173–180

Turin, L., Warner, A.E. 1977. Carbon dioxide reversibly abolishes ionic communication between cells of early amphibian embryo. *Nature* (*London*) **270:**56–57

Turin, L., Warner, A. 1980. Intercellular pH in early *Xenopus* embryos: Its effect on current flow between blastomeres. *J. Physiol.* (*London*) **300:**489–504

Received 2 March 1983; revised 27 May 1983